

## *Numerical Analysis of Salt Intrusion into Aquifer by Eulerian Lagrangian Finite Element Method*

Makoto NISHIGAKI \*, Teddy SUDINDA \*\*, Tomoyuki HISHIYA \*\*\*, Iichiro KOHNO \*

(Received September 30 , 1993)

### SYNOPSIS

In this paper, method of Eulerian Lagrangian numerical analysis is used to described Advection-Dispersion phenomena. The influence of concentration to the density of fluid is considered. A laboratory model of a two dimensional confined aquifer containing an isotropic, homogeneous porous medium (Hosokawa et.al 1989) was used to validate the applicability of Advection-Dispersion of numerical analysis with steady and unsteady state condition [1].

### 1. INTRODUCTION

The population growth of the world, the coastal region have become more densely settled. The increased use of freshwater supplies in these coastal region has upset the long existing dynamic balance between the fresh water flow to the ocean. The Ghyben Herzberg static equilibrium principle was the first formulation for the extent of salt intrusion. Rate of mixing in the porous media for fresh and salt water depends on the pore system Geometry and the seepage velocities. This mixing proces occurring in porous media has been called dispersion. The local velocity pattern in the ground water is the mechanism causing dispersion, thus the extent of the transition zone between fresh water and salt water will be governed by seepage velocities that occur in this region. And also a balance equation for salt is needed to account for the mass transport processes of Advection and Dispersion.

A number of researcher have been active in the area of seawater intrusion. Such as Henry (1964) applied of the analytical hydraulic approach, and experimentally used a Hele show model, and they was study a confined aquifer with sharp interface [2]. The one dimensional transient toe problem was modeled by Shamir and Dagan (1971) and by using sharp interface with hydraulic approach and finite difference method. They was assumed the interface is a well defined line, the effect of dispersion between the moving fresh and salt water is neglected and they also assumed the hydraulic head along vertical line in the fresh

\* Department of Civil Engineering

\*\* Graduate Student in Department of Civil Engineering

\*\*\* D I A Consultant

and saltwater zone is constant [3]. S. Costa and J. Wilson presented transition zone between fresh water and salt water, Where mixing and dispersion phenomena occurs is assumed quite narrow when compared with the overall saturated thickness of the aquifer formation. Therefore in this case they were analysed as immiscible interface [4]. I. Kono and M. Nishigaki (1982) presented Finite Element Analysis of unsteady condition for interface between salt and freshwater in coastal aquifer and they have been compared with laboratory model test ( small tube net model) [5]. M. Nishigaki et.al (1992) presented Advection Dispersion by Eulerian Lagrangian Finite Element Method and they have been compared with analytical solutions [6].

In this paper, we will show the Eulerian Lagrangian Finite Element Method to analysis the phenomena of salt water intrusion, and demonstrate the validity of this method by comparing with the experimental result that is presented Hosokawa et.al.

## 2. GOVERNING EQUATION

The governing equations are the Darcy Equation, the continuity equation for the fluid, the continuity equation for the dissolved salt, and a constitutive equation relating fluid density to salt concentration. Density dependent fluid transport problems is to take pressure as the basic unknown in the fluid continuity equation (Segol, Pinder and Gray, 1975) [7]. The general Darcy equation then takes the form :

$$V_d = -k_{ij} \left( \frac{\partial h}{\partial x_i} + \left( \frac{\rho}{\rho_f} - 1 \right) n_j \right) \quad \dots\dots\dots (1)$$

Where :  $V_d$  = darcy velocity

$k_{ij}$  = permeability tensor

$h$  = total head

$x_i$  = coordinates direction

$\rho$  = density

$\rho_f$  = density of fresh water

$n_j$  = normal vector

$$h = \psi + z \quad \text{and} \quad \psi = p/\rho_f.g + z \quad \dots\dots\dots (2)$$

Where  $\psi$  = water head

$g$  = gravitational acceleration

$z$  = elevation above datum

$p$  = pressure head

Substituting Eq.(2) into Eq.(1) yields

$$V_d = -k_{ij} \left( \frac{\partial \psi}{\partial x_i} + n_j + \left( \frac{\rho}{\rho_f} - 1 \right) n_j \right) = -k_{ij} \left( \frac{\partial \psi}{\partial x_i} + p_r . n_j \right) \quad \dots\dots\dots (3)$$

and  $p_r = \rho/\rho_f$

The continuity equation for the fluid can be written in the form

$$\frac{1}{\rho} \frac{\partial}{\partial t} (\rho \cdot n \cdot S_w) + \frac{\partial}{\partial x_i} (-k_{ij} (\frac{\partial \psi}{\partial x_i} + \rho r \cdot n_j)) = 0 \quad \dots\dots\dots (4)$$

$n$  = porosity                       $S_w$  = degree of saturation

Substituting a constitutive equation relating fluid density to salt concentration ( $\rho = \rho_f (1 + \gamma C)$ ) and the Eq.(3) into Eq.(4) yield :

$$\frac{\rho_f \cdot \gamma \cdot \theta}{\rho} \cdot \frac{\partial C}{\partial t} + (\alpha \cdot S_s + C_s(\theta)) \frac{\partial \psi}{\partial t} - \frac{\partial}{\partial x_i} (k_{ij}^{(s)}(\theta) \frac{\partial \psi}{\partial x_i} + k_{i3} \cdot k_r(\theta) \rho r) = 0 \quad \dots\dots\dots (5)$$

Where  $\rho$  = density of fluid,  $\rho_f$  = density of fresh water

$\theta$  = moisture content,  $C$  = concentration

$S_s$  = specific Storage,  $\Psi$  = pressure head

$k_{ij}$  = permeability tensor

And then the continuity equation for dissolved salt ( advection dispersion equation ) takes the form

$$R \cdot \theta \cdot \rho \cdot \frac{\partial C}{\partial t} = \nabla \cdot (\theta \cdot \rho \cdot D \cdot \nabla C) - \theta \cdot \rho \cdot V_s \cdot \nabla \cdot C - \theta \cdot \lambda \cdot R \cdot C + Q_p C^* \quad \dots\dots\dots (6)$$

Where  $R = (1 + \rho_s/n \cdot k_d)$

$D$  = dispersion tensor

$V = V_d/\theta$  ;  $V_d$  = darcy velocity

$\theta$  = moisture content,  $n$  = porosity

Eq.(5) and Eq.(6) are coupled through the density and the velocity. Therefore they must be solved either simultaneously or iteratively.

### 3. BOUNDARY CONDITION

The basic system is shown in Fig.1. The lateral boundaries at both the seaward side (left) and the landward side (right) are located at point where the concentration is constant. The bottom and upper of aquifer is impermeable. The boundary condition are as follows :

- Bottom Boundary

$$Q_n = 0$$

$$\frac{\partial C}{\partial y} = 0$$

- Upper boundary

$$Q_n = 0$$

$$\frac{\partial C}{\partial y} = 0$$

- Seaward boundary

$$h = (H_s - y) \rho_s / \rho_f$$

$$C = 1$$

$$\frac{\partial C}{\partial x} = 0$$

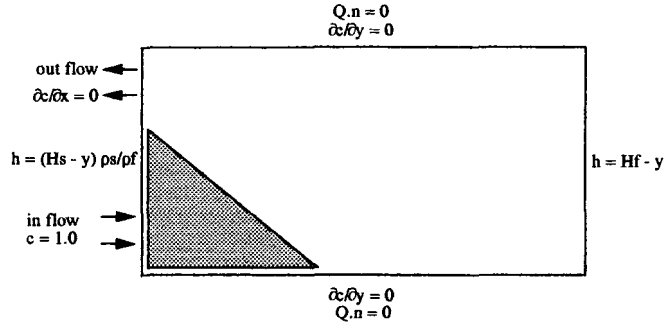


Fig. 1 Boundary Condition of Salt Intrusion Model

- Landward Boundary

$$h = H_f - y$$

$$C = 0$$

#### 4. FINITE ELEMENT SOLUTION

The solution of the seawater intrusion problem requires a highly efficient numerical scheme. The reason is that intrusion zones may extend for considerable distance, and long time periods may be required to reach equilibrium.

We will give the final matrix equation for the finite element solution. The matrix equation for fluid flow is of the form :

$$[A_{nm}] \dot{\psi}_m + [F_{nm}] \frac{\partial \psi_m}{\partial t} + [X_{nm}] \frac{\partial C_m}{\partial t} - \{Q_n\} - \{B_n\} = 0 \quad \dots\dots\dots (7)$$

Where :  $[A_{nm}]$  : the conductivity matrix

$[F_{nm}]$  : storage matrix

$[X_{nm}]$  : storage matrix

$\{Q_n\}$  : contains the known boundary fluxes

$\{B_n\}$  : contain the buoyancy term

Solution with time step  $\Delta t$ , the time derivatives can be approximated by

$$\frac{\partial \psi_m}{\partial t} = \frac{\psi_m^{k+1} - \psi_m^k}{\Delta t^k}$$

$$\frac{\partial C_m}{\partial t} = \frac{C_m^{k+1} - C_m^k}{\Delta t^k}$$

$$\psi_m^{k+1} = \omega \cdot \psi_m^{k+1} + (1 - \omega) \psi_m^k$$

Where  $\omega = 1/2$  = central difference

$\omega = 1$  = backward difference

$k$  = time step

$$\Delta t^{k+1} = t^{k+1} - t^k$$

the matrix Eq. (7) then becomes :

$$\left( \frac{F_{nm}^{k+1/2}}{\Delta t^k} + \omega A_{nm}^{k+1/2} \right) \psi_m^{k+1} = Q_n^{k+1} - B_n^{k+1/2} - \frac{C_m^{k+1} - C_m^k}{\Delta t^k} X_{nn}^{k+1/2} + \left( \frac{F_{nm}^{k+1/2}}{\Delta t^k} - (1 - \omega) A_{nm}^{k+1/2} \right) \psi_m^k \quad \dots\dots\dots (8)$$

The Eq. (8) is portioned according to unknown and known nodal values of  $\psi_m^k$  and the equations. Corresponding to the known values are removed, the remaining equations can then be solved for  $\{\psi_m^{k+1}\}$ . The matrix equation for salt transport is of the form

$$\left( \frac{C_n^{k+1} - C_n^k}{\Delta t} \right) [W_{nm}] - \left( \frac{\tilde{C}_n^{k+1} - \tilde{C}_n^k}{\Delta t} \right) [W_{nm}] + [G_{nm}] \cdot C_m + [H_{nm}] C_m + (C_n - \tilde{C}_n) [L_n] + [U_n] = 0 \quad \dots\dots\dots (9)$$

Where  $[W_{nm}]$  : mass storage matrix

$[G_{nm}]$  : transport matrix which expresses the convective and dispersive properties of system

$[L_n]$  : contain the known retardation coefficient

$[U_n]$  : contain the known boundary fluxes

$\{C\}$  : vector of nodal concentration

The latter again approximated by

$$C_m = \omega C_m^{k+1} + (1 - \omega) C_m^k$$

$$\tilde{C}_m = \omega \tilde{C}_m^{k+1} + (1 - \omega) \tilde{C}_m^k$$

Where  $\omega = 1/2$  = central difference

$\omega = 1$  = backward difference

The matrix equation becomes

$$\left\{ \omega (G_{nm} + N_{nm} + L_n) + \frac{W_{nm}}{\Delta t} \right\} C_n^{k+1} = -(1 - \omega) (G_{nm} + N_{nm} + L_n) C_n^k + \left( \omega L_n + \frac{W_{nm}}{\Delta t} \right) \tilde{C}_n^{k+1} + (1 - \omega) L_n \tilde{C}_n^k - U_n \quad \dots\dots\dots (10)$$

Equation (10) is partitioned in the same way as (8) and the equation corresponding to the known value of

$\{C\}_n^k$  are eliminate. The remaining equations are solved for  $\{C\}_n^{k+1}$ .

The major part of the computational effort is consumed in the solution of the matrix equations.

To solve (8) and (10) we use gaus elimination. The model tested by comparison with experimental result that presented Hosokawa et.al (1989).

## 5. COMPARISON OF NUMERICAL ANALYSIS AND EXPERIMENTAL RESULT

### 5.1 MODEL OF NUMERICAL ANALYSIS

In this paper model of experimental Hosokawa et.al (1989) is used to the model of numerical analysis. It is, can be shown in Fig.(2). The model consist of 5000 element and 5151 node point, length 100 cm, width 50 cm and size of element 1 cm, it is shown in Fig.(3). Boundary condition can be shown in Fig.

(1) .The constant parameter of the system are :

Transversal dispersivity ( $\alpha_T$ ) = 0.0050 cm

Longitudinal dispersivity ( $\alpha_L$ ) = 0.2196 cm

Porosity ( $n$ ) = 0.406

Permeability Coefficient ( $k$ ) = 3.5 cm/sec

Elevation of salt water (left side) = 53 cm

Elevation of fresh water (right side) for steady state condition = 54.7 cm

Elevation of fresh water (right side) for unsteady state condition = 54.7 cm fall down become 53.5 cm suddenly.

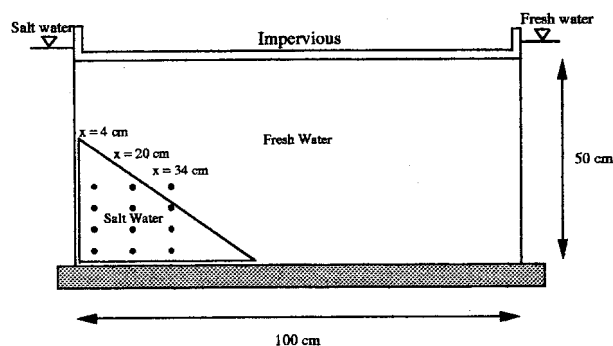


Fig. 2 Experimental Model of Salt Intrusion

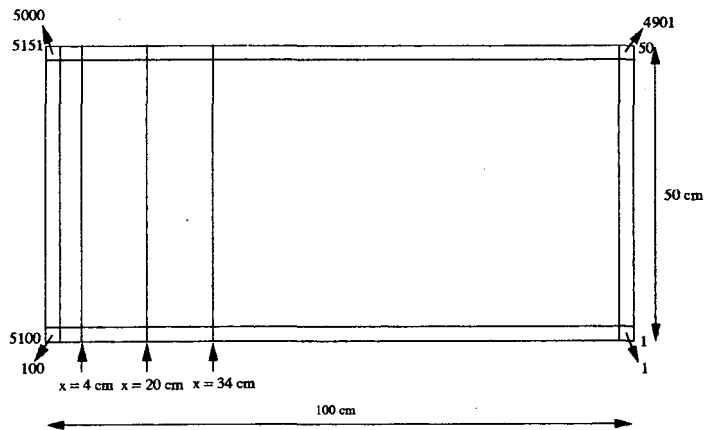


Fig. 3 Model of Two Dimensional Salt Intrusion Problem (size each element = 1 cm)

## 5.2 RESULT OF NUMERICAL ANALYSIS

Comparing the concentration contours of numerical analysis and experimental result for steady and unsteady state condition can be shown in Fig.(4),(5),(6),(7). And the results of numerical analysis can be shown in Fig.(8),(9),(10), which depict the result of steady state condition and Fig.(11),(12),(13) depict the results of unsteady state condition. Then Fig.(8) shows the correlation of concentration and y coordinate at position  $x = 4$  cm. Where the solid line show the numerical analysis and dots is experimental result. From this figure, it is clear that the numerical result well agree with the experimental data. Fig.(9) and Fig.(10) shows the correlation of concentration and y coordinate at position  $x = 20$  cm and at position  $x = 34$  cm. From this figure also we obtained the result agree very well. Afterwards, Fig.(11) shows a vertical distribution of concentration at the position of  $x = 20$  cm and at time = 1 minute in unsteady state condition. The solid line shows the result of numerical analysis and dots show the result of experimental. And Fig.(12) shows the distribution of concentration at  $x = 20$  cm and at time = 3 minutes in unsteady state condition, also the result ( $t = 5$  minutes) is shown in Fig. (13). The concentration contour lines for steady state condition can be shown in Fig.(14) and the results for unsteady state condition are shown in Fig.(15),(16),(17), at time = 1 minute, time = 3 minutes and time = 5 minutes respectively.

## 6. CONCLUSION

The numerical results of steady and unsteady state salt intrusion have been shown and there were compared with experimental results that were presented by Hosokawa et.al (1989). It become clear that the results of numerical analysis well agree with the experimental results. From concentration contour line the transition zone can be shown the interface between fresh and saltwater. This zone is created by the flow field and effect of hydrodynamics dispersion. In this paper fresh and seawater are treated as miscible fluids, therefore effect of hydrodynamics dispersion become easily considerable.

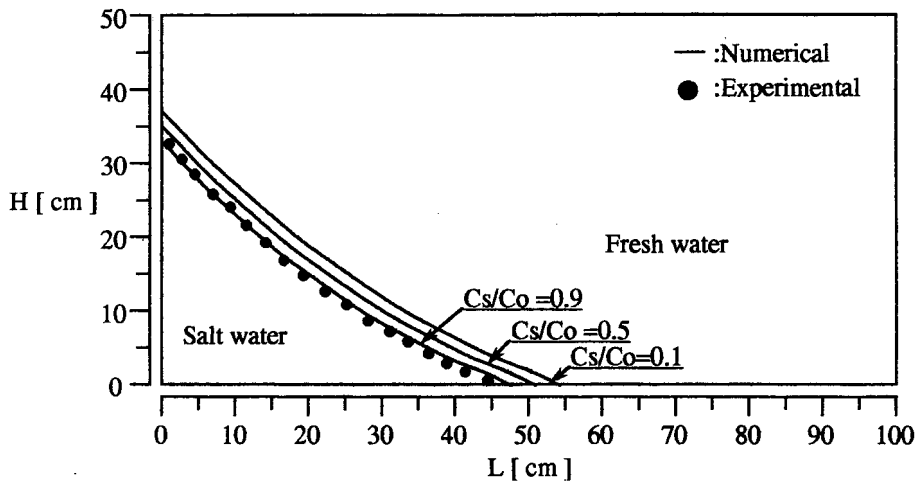


Fig. 4 Comparison Concentration Contour Between Numerical and Experimental in Steady State Condition

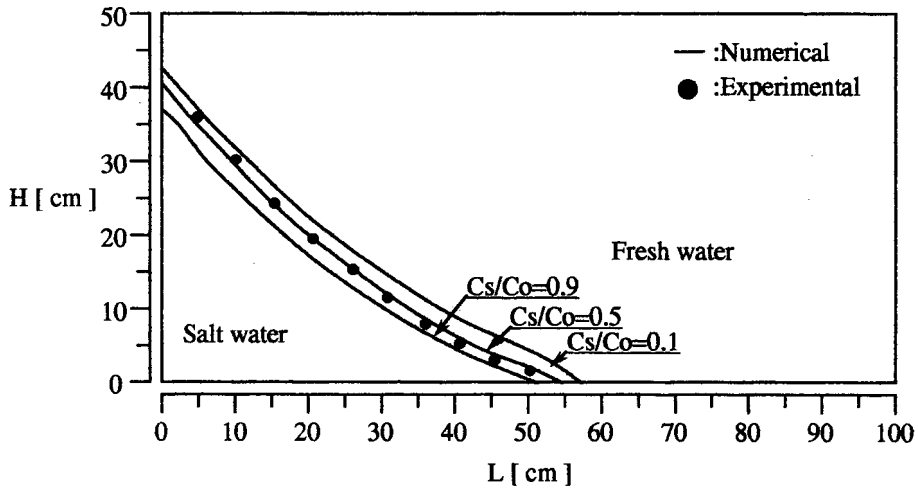


Fig. 5 Comparison Concentration Contour Between Numerical and Experimental in Unsteady State Condition ( $t = 1$  minute)



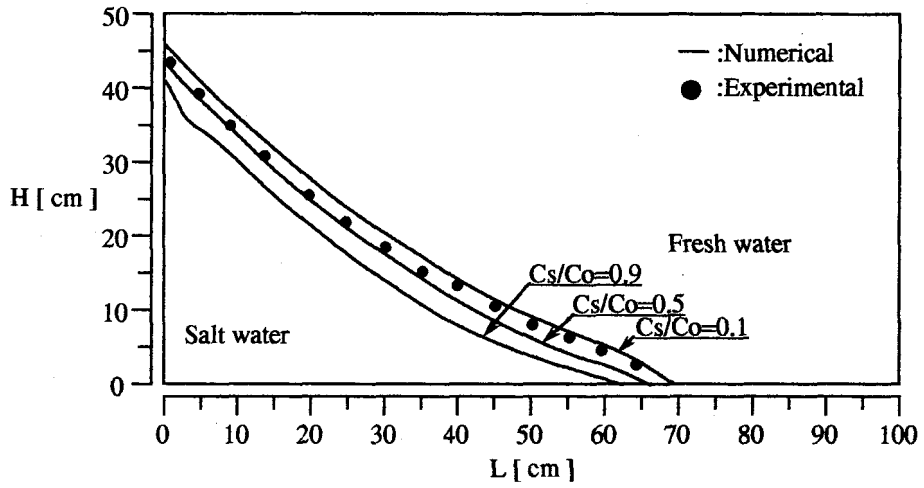


Fig. 6 Comparison Concentration Contour Between Numerical and Experimental in Unsteady State Condition ( $t = 3$  minutes)

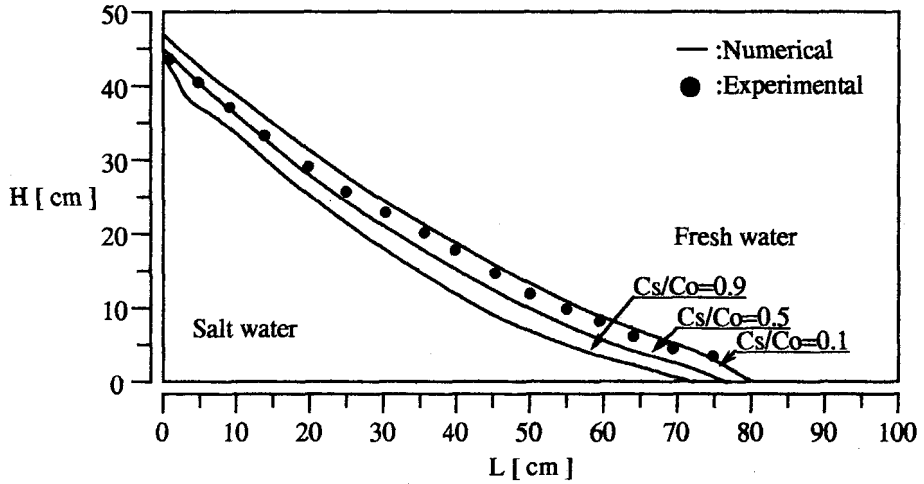


Fig. 7 Comparison Concentration Contour Between Numerical and Experimental in Unsteady State Condition ( $t = 5$  minutes)

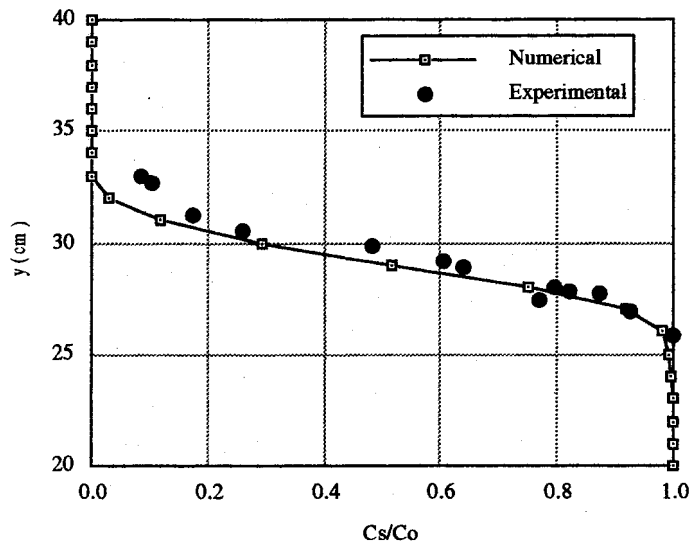


Fig. 8 Comparison of Numerical and Experimental Result in Steady State Condition ( $x=4\text{cm}$ )

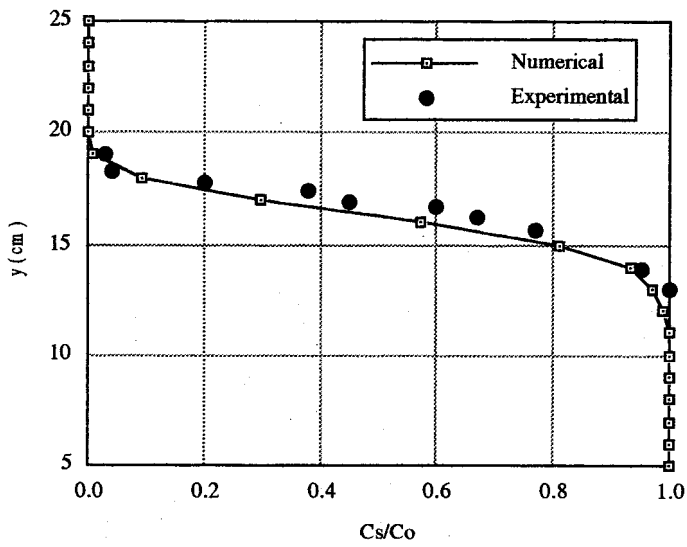


Fig.9 Comparison of Numerical and Experimental Result in Steady State Condition ( $x=20\text{cm}$ )

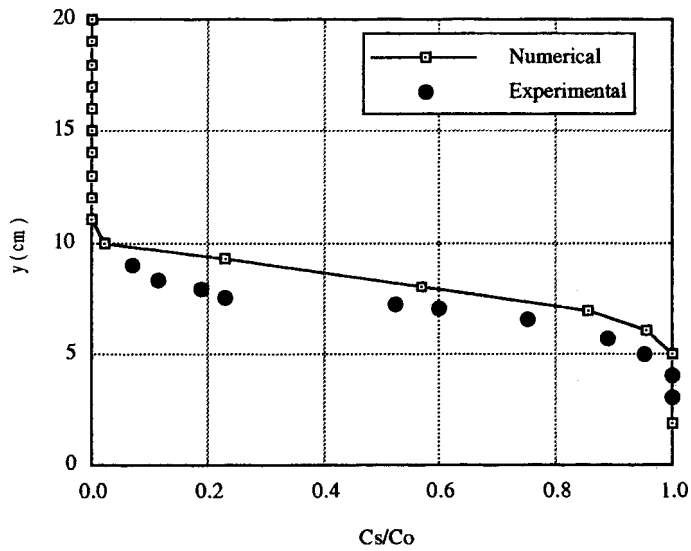


Fig.10 Comparison of Numerical and Experimental Result in Steady State Condition ( $x=34\text{cm}$ )

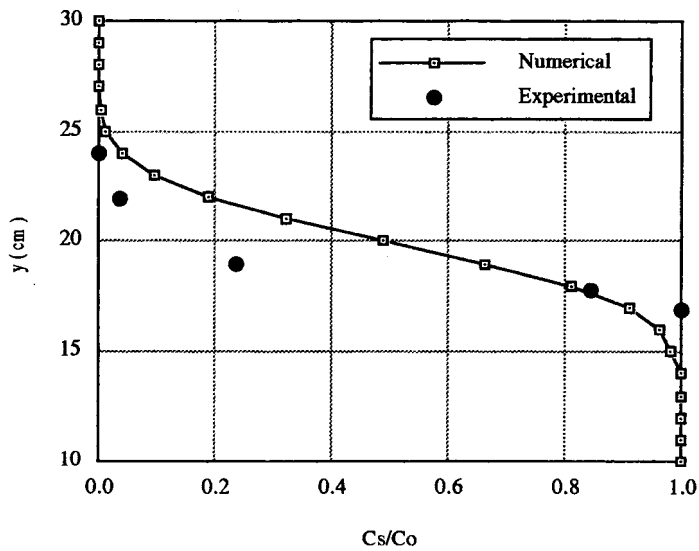


Fig. 11 Comparison of Numerical and Experimental Result in Unsteady State Condition ( $t = 1\text{minutes}$ ,  $x = 20\text{ cm}$ )

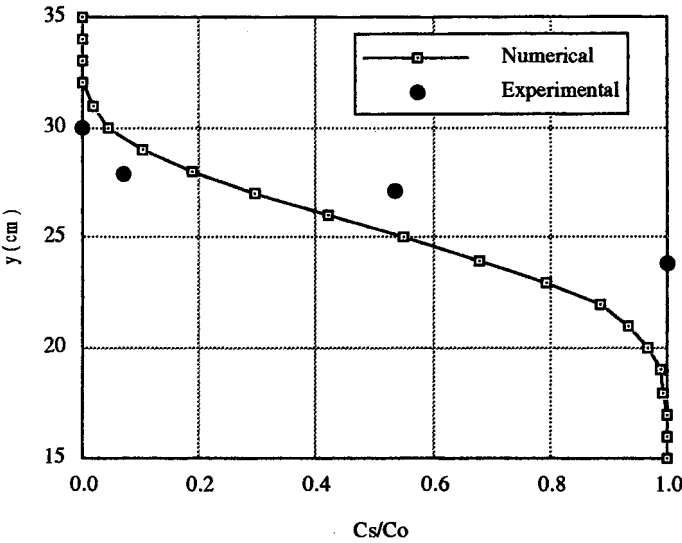


Fig. 12 Comparison of Numerical and Experimental Result in Unsteady State Condition ( t = 3 minutes, x = 20 cm )

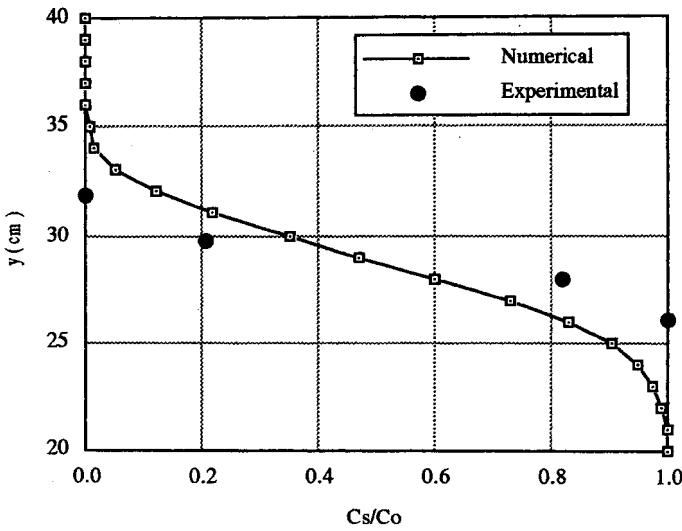


Fig. 13 Comparison of Numerical and Experimental Result in Unsteady State Condition ( t = 5 minutes, x = 20 cm )

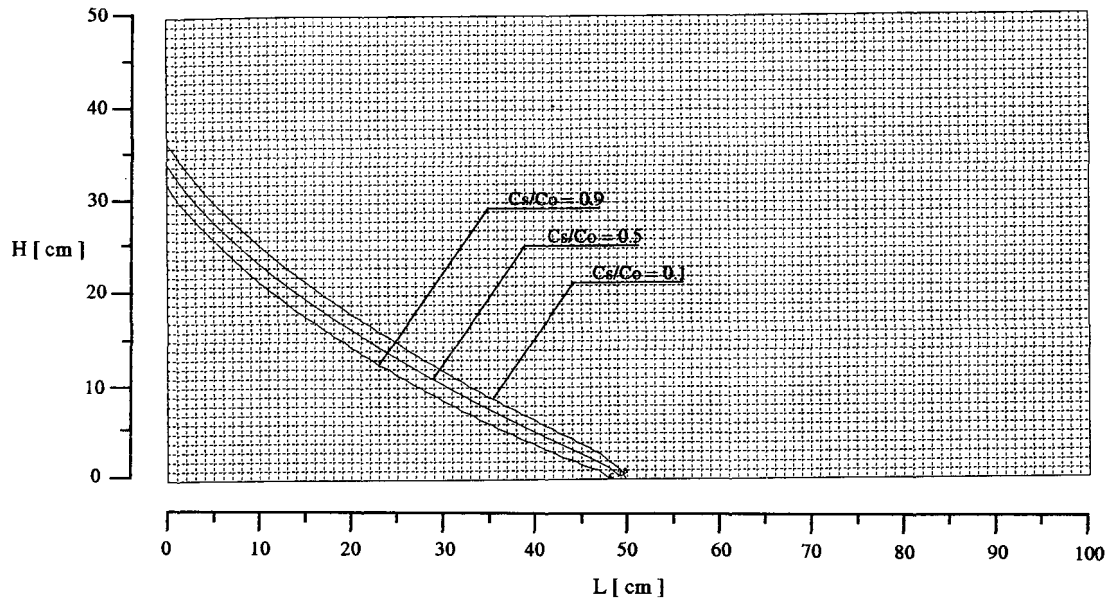


Fig. 14 Concentration Contour lines of Steady State Condition

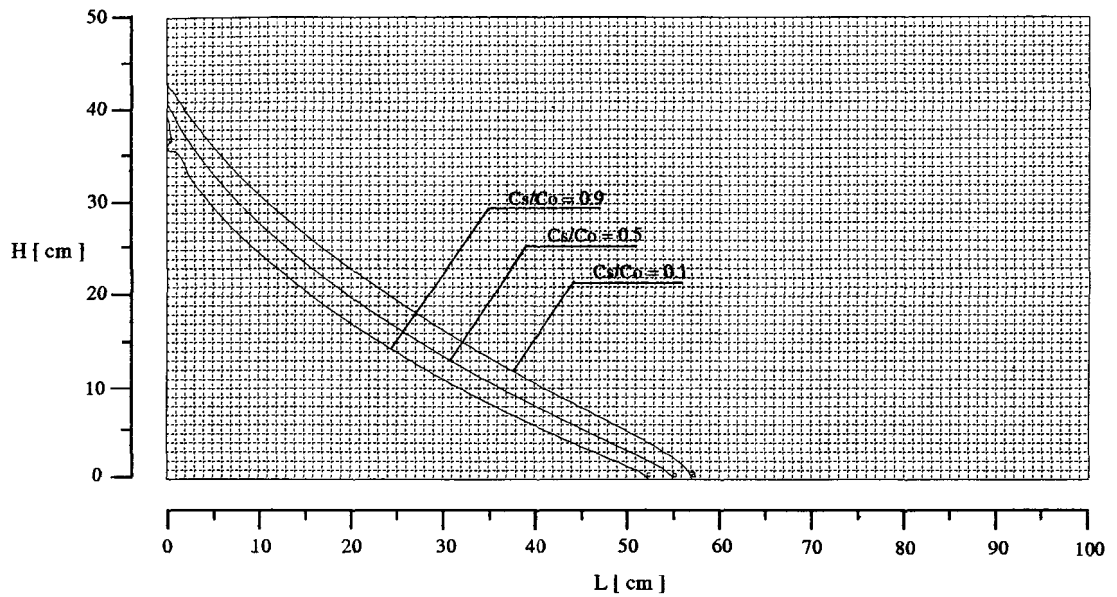


Fig. 15 Concentration Contour lines of Unsteady State Condition at Time = 1 Minute

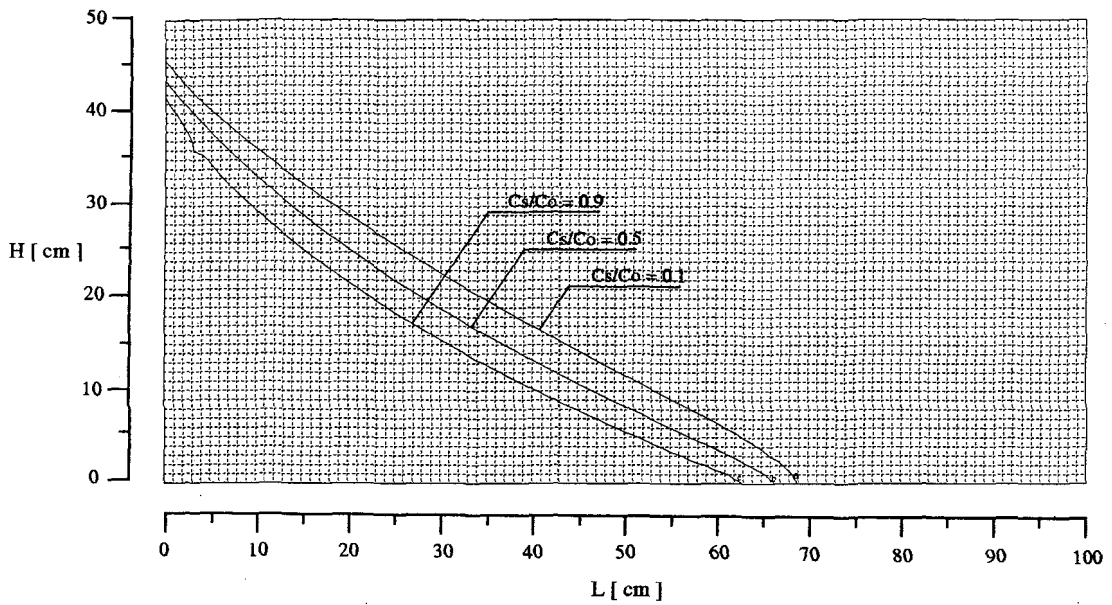


Fig. 16 Concentration Contour lines of Unsteady State Condition at Time = 3 Minutes

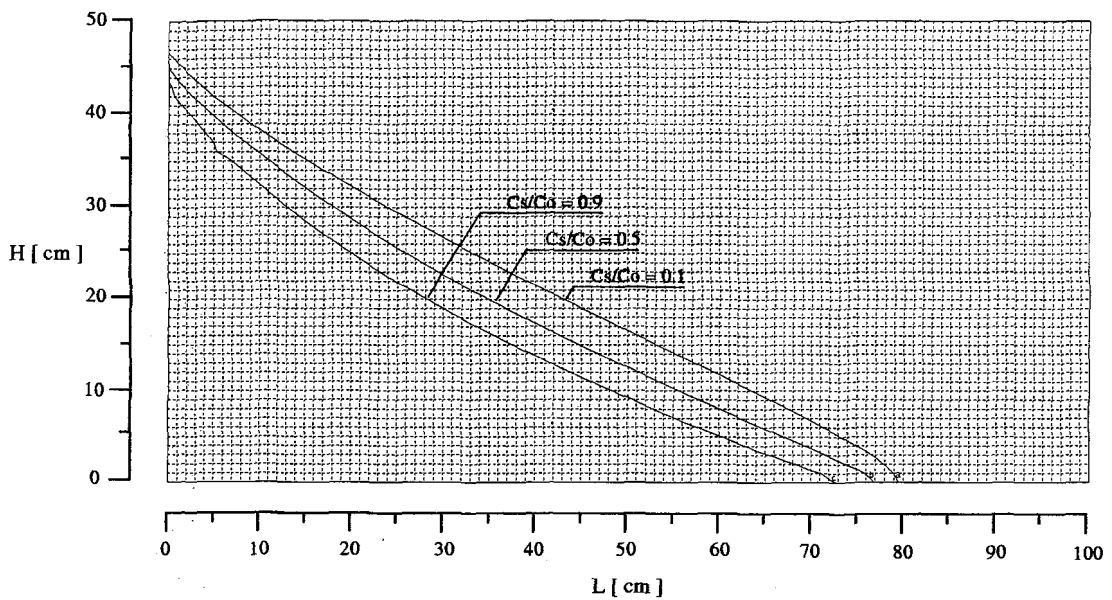


Fig. 17 Concentration Contour lines of Unsteady State Condition at Time = 5 Minutes

# REFERENCES :

- [1] T. Hosokawa, Estimation of Transverse Dispersivity in the Mixing Zone Fresh - Salt Groundwater, Calibration and Reliability in Groundwater Modeling.
- [2] H.R Henry, Effect on Dispersion Salt Encroachment in Coastal Aquifer, U,S Geological Survey Water Supply paper 1613 - C, pp C 71 - C 84, 1964.
- [3] U. Shamir and Dagan, Motion of the Seawater Interface in Coastal Aquifers : A Numerical Solution , Water Resources Research Vol.7 no. 3, pp.644 - 657, June 1971.
- [4] A. G Sada Costa and J Wilson, Coastal Seawater Intrusion A Moving Boundary Problem, pp. 2.209 - pp. 2.218.
- [5] I. Kono and M. Nishigaki, Finite Element Analysis of Salt Water Intrusion Nonsteady Seepage, Memoirs of the School of Engineering, Okayama University, Vol. 16-2, pp. 89 - 99 , November 1982.
- [6] M. Nishigaki, Teddy Sudinda, T. Hishiya and I. Kohno, Advection Dispersion by Eulerian Lagrangian Finite Element Method, Memoirs of the Faculty of Engineering, Okayama University, Vol.27-1, pp. 93-105, November 1992.
- [7] G. Segol, G.F. Pinder, W.G. Gray, A Galerkin Finite Element Technique for Calculating the Transient Position of the Saltwater Front, Water Resources Research, Vol 11-2, pp.343-347, April 1975.